IEEE Access
Multidisciplinary ⋮ Rapid Review ⋮ Open Access Journal

Received 18 January 2023, accepted 20 February 2023, date of publication 27 February 2023, date of current version 2 March 2023.

Digital Object Identifier 10.1109/ACCESS.2023.3249968

RESEARCH ARTICLE

CSRR DGS-Based Bandpass Negative Group Delay Circuit Design

QIZHENG JI[1,2], TAOCHEN GU[3], (Student Member, IEEE), ZHILIANG GAO[4], MING YANG[4], YAFEI YUAN[4], HONGYU DU[3], (Student Member, IEEE), FAYU WAN[3], (Senior Member, IEEE), NOUR MOHAMMAD MURAD[5], (Member, IEEE), GLAUCO FONTGALLAND[6], (Senior Member, IEEE), HUGERLES S. SILVA[7,8], (Member, IEEE), AND BLAISE RAVELO[3], (Member, IEEE)

[1]National Key Laboratory on Electromagnetic Environment Effects, Army Engineering University, Shijiazhuang 050003, China
[2]Beijing Institute of Spacecraft Environment Engineering, Beijing 100094, China
[3]School of Electronic and Information Engineering, Nanjing University of Information Science and Technology (NUIST), Nanjing 210044, China
[4]Beijing Orient Institute for Measurement and Test, Beijing 100086, China
[5]PIMENT, Network and Telecom Laboratory, Institute Universitaire de Technologie, University of La Réunion, 97410 Saint Pierre, France
[6]Applied Electromagnetic and Microwave Laboratory, Federal University of Campina Grande, Campina Grande 58429, Brazil
[7]Departamento de Eletrónica, Telecomunicações e Informática, Instituto de Telecomunicações, Universidade de Aveiro, Campus Universitário de Santiago, 3810-193 Aveiro, Portugal
[8]Department of Electric Engineering, University of Brasília (UnB), Federal 70910-900, Brazil

Corresponding author: Taochen Gu (taochen_gu@nuist.edu.cn)

This work was supported in part by the National Key Research and Development Program of China under Grant 2022YFE0122700; and in part by the Electrostatic Research Foundation of Liu Shanghe Academicians and Experts Workstation, Orient Institute of Measurement and Test, under Grant BOIMTLSHJD20221004.

ABSTRACT The unfamiliar negative group delay (NGD) circuit is the less familiar function for most of RF and microwave design engineers. Among the existing types, the bandpass (BP) NGD type circuits are the most convenient for the wireless communication microwave technology. Therefore, it is particularly important to explore different microwave circuit topologies operating as BP-NGD function. An innovative design of BP-NGD topology constituted by defected ground structure (DGS) with complementary split ring resonator (CSRR) is developed in the present paper. The DGS-based BP-NGD structure design method is introduced in function of the CSRR geometrical elements followed by S-parameter parametric analyses. As proof-of concept (POC), the design method of the proposed BP-NGD passive fully distributed circuit is described. The effectiveness of the BP-NGD structure and the test feasibility are investigated by implementing two different prototypes represented by single- and double-wing DGS passive circuits. It is observed that significant BP-NGD function performances were validated by well-correlated simulations and measurements showing -1.9 ns NGD value around the center frequency, 2.46 GHz over 31 MHz NGD bandwidth. In addition, the tested BP-NGD prototypes present insertion loss better than 4 dB and reflection loss better than 16.7 dB. Because of its potential integration, the investigated BP-NGD circuit is potentially useful for the communication system performance improvement for example via delay effect reduction in the RF and microwave devices.

INDEX TERMS Defected ground structure (DGS), design method, microwave circuit, bandpass negative group delay (BP-NGD) function, NGD analysis.

I. INTRODUCTION

The negative group delay (NGD) circuits are proposed in literatures to solve the delay problems which limit the RF microwave device performance. For example, in [1] and [2], it uses NGD RLC-resonant network implementation in feed-forward amplifier. It enables to increase the amplifier efficiency and decreases the circuit size. In [3] and [4], the NGD circuit was also used to overcome the main drawback of serially fed arrays namely the beam squint. A 4° phase variation

The associate editor coordinating the review of this manuscript and approving it for publication was Wenjie Feng.

between the adjacent antennas provides a maximum 2° beam squint, an almost 75% beam squint reduction compared to a serially fed array without using an NGD circuit.

However, the RLC NGD passive circuits suffer high attenuation losses which may reach 20 dB and the distributed NGD circuits have large size problem. To alleviate the circuit size problem, defected ground structure (DGS) technology is used. The main strengths to make DGS to be potentially integrable are the design simplicity and easiness of miniaturization [5]. Because of these benefits, the DGSs have been extensively used to design microwave circuits. An effective technique of second and third harmonic suppression for a Wilkinson power divider by using an asymmetric spiral DGS was developed [6]. The asymmetric DGS characteristics were modeled by two parallel RLC resonance circuits in cascade [6]. It was reported that using asymmetric DGS, the size of a quarter-wave line can be reduced by 9.1%. It was also investigated that the optimization of DGS geometries allows to minimize the size defect of circular patch [7], [8], [9]. The 35% size reduction and highest order of achievable suppression of cross-polarized (XP) radiations are based on the DGS strategic shaping [7]. The asymmetrically conFig.d antenna designs have been emphasized with a view for addressing the asymmetry in modal fields [7]. This antenna characterization performance was examined in X-band and experimentally verified with promising achievement of 16-18 dB XP suppression over H-plane [7]. In addition to these classical microwave function designs, the DGS was also exploited to design the unfamiliar bandpass (BP) NGD function [10], [11]. It was found that the defected microstrip structures were used to design dual-band NGD circuits (NGDCs) operating between 3.46-3.58 GHz and 5.10-5.20 GHz [10]. Similar to the classical functions reported in [5], [6], [7], [8], and [9], compact NGD microstrip passive circuits with DGSs were designed [10], [11].

Behind this progressive NGD design investigation, further research works were required about the design of NGD microwave circuits by illustrating the adequate characterization techniques required by RF and microwave standards.

At present, most of BP-NGD RF and microwave circuits are designed by exploring basic topologies constituted by microstrip resonators coupled with microstrip lines [23], [24], [25]. This kind of BP-NGD topologies is usually connected to both ends of the circuit to be balanced in cascaded form. The disadvantage of those design is that the microstrip resonant structure will take up too much space on the PCB board and increase the size of the circuit while causing radiation interference to other transmission lines (TLs).

The novelty of the present paper compared to the NGD research ones available in the literature [12], [13], [14], [15], [16], [17], [18], [19], [20], [23], [24], [25] concerns the design method of complementary split ring resonator (CSRR) based DGS compact NGDC. The DGS BP-NGD circuit is easy to be integrated into other classical microwave devices familiarly available in the transceiver system. The flexibility of the BP-NGD novel topology under study is its implementation on the back side of the printed circuit board (PCB) and at the front side there is only one TL. The DGS BP-NGD circuit under study operates challengingly under low insertion loss, good reflective loss performance and small size. Two different topologies of single- and double-wing DGSs will be explored. The paper is organized in four main sections as follows:

- Section II explains generally the main specifications, parameters and the design method of the BP-NGD microwave passive circuits.
- Section III describes the application BP-NGD design and test method to an innovative single wing CSRR circuit implemented with DGS microstrip structure. The designability is validated by a prototype of single-wing DGS proofs-of-concept (POC). The BP-NGD effectiveness is validated by comparison of full wave simulations from commercial tools and S-parameter measurement.
- To improve the BP-NGD performance, a two-wing DGS circuit will be analyses in Section IV. To confirm the BP-NGD effectiveness, a comparison study with BP-NGD circuit performances available in the literature will be discussed.
- Then, Section V ends the paper with a conclusion.

II. SPECIFICATION AND DESIGN METHOD OF BP-NGD MICROWAVE PASSIVE CIRCUIT

The design approach of BP-NGD microwave passive circuits is practically analog to the classical electronic circuits (filters, phase shifters, couplers, . . .). This section explores the design methodology of BP-NGD microwave circuit. The analytical approach based on two-port S-parameters will be explored. The specification parameters are defined.

A. ANALYTICAL SPECIFICATIONS OF BP-NGD MICROWAVE CIRCUIT

The tradition of RF and microwave engineering guides to the characterization of all two-port microwave circuit with the consideration of S-parameters. For the cases of symmetric microwave circuit, the circuits are modeled by an equivalent 2-D S-matrix written as:

$$\left[S^{NGD}(j\omega)\right] = \begin{bmatrix} S_{11}^{NGD}(j\omega) & S_{21}^{NGD}(j\omega) \\ S_{21}^{NGD}(j\omega) & S_{11}^{NGD}(j\omega) \end{bmatrix} \quad (1)$$

where $j\omega$ is the complex angular frequency variable. The associated group delay (GD) is mathematically defined by:

$$GD(\omega) = -\partial\varphi(\omega)/\partial\omega \quad (2)$$

with the transmission phase:

$$\varphi(\omega) = \arg\left[S_{21}^{NGD}(j\omega)\right] \quad (3)$$

is the transmission phase. The BP-NGD performance is quantified by the parameters:

- Around the NGD center frequency:

$$\omega_0 = 2\pi f_0 \quad (4)$$

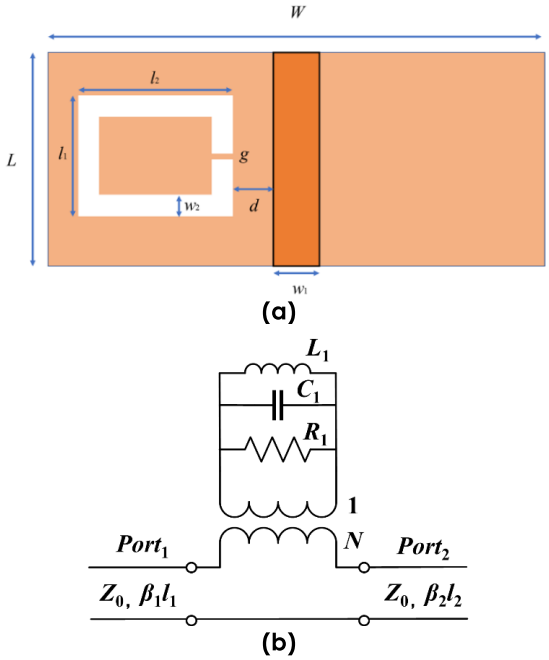

FIGURE 1. Single-wing DGS planar design: (a) top view of the overall circuit and (b) equivalent circuit.

- NGD value:

$$GD(\omega_0) = \min\left[GD(\omega)\right] \tag{5}$$

- NGD bandwidth:

$$\Delta\omega = \omega_2 - \omega_1 \tag{6}$$

where GD $(\omega_1 < \omega < \omega_2) < 0$ knowing the cut-off frequencies defined by:

$$GD(\omega_1) = GD(\omega_2) = 0. \tag{7}$$

- Transmission coefficient:

$$S_{21}^{NGD}(\omega_0) = \left|S_{21}^{NGD}(j\omega_0)\right| \tag{8}$$

- And reflection coefficient:

$$S_{11}^{NGD}(\omega_0) = \left|S_{11}^{NGD}(j\omega_0)\right| \tag{9}$$

This BP-NGD analytical specifications will serve to design the DGS BP-NGD topology as described in the following section.

B. THEORETICAL APPROACH OF DGS-BASED BP-NGD MICROWAVE CIRCUIT

The theory of the DGS-based BP-NGD prototype is introduced in this section.

1) 2-D DESIGN AND EQUIVALENT CIRCUIT

Figs. 1 introduce the BP-NGD design of microstrip planar passive and microwave circuit representing a single-wing DGS POC. Our circuit prototype is constituted by a microstrip TL and split ring resonator (SRR) etched ground plane.

As seen in Fig. 1(a), the circuit is geometrically designed with width, W, and length, L. The TL was designed with characteristic impedance equal to the terminal load reference impedance, $Z_0 = 50\ \Omega$. Fig. 1(a) illustrates the DGS wing design. It consists of a SRR having physical parameters, $l_{1,2}$, w_2 and space, g, which is placed at distance, d, in left of the microstrip line. In order to better analyse the group delay performance, we convert the DGS POC to the equivalent lumped RLC-network shown in Fig. 1(b). The SRR is represented by R_1, C_1 and L_1 in parallel. The coupling between SRR and microstrip line is represented by a transformer with turn ratio N.

2) S-PARAMETER AND GD

Under this circuit configuration, the SRR angular frequency can be written as:

$$\omega_0 = \frac{1}{\sqrt{L_1 C_1}} \tag{10}$$

The quality factor of unloaded SRR can be written with (R_1, L_1, C_1) couple of parameters:

$$Q = \frac{R_1}{\omega_0 L_1} = \omega_0 R_1 C_1 \tag{11}$$

The coupling coefficient can be expressed as:

$$g = \frac{Q}{Q_e} = \frac{N^2 R_1}{2Z_0} \tag{12}$$

where Q_e is the quality factor of SRR loaded on the microstrip line TL. We know that the equivalent impedance of the R, L, and C parallel network is defined by:

$$Z(j\omega) = \frac{N^2 R_1}{1 + j\omega R_1 C_1 - j\frac{R_1}{\omega L_1}} \tag{13}$$

which can be rewritten as:

$$Z(j\omega) = \frac{N^2 R_1}{1 + jQ\frac{\omega^2 - \omega_0^2}{\omega\omega_0}}. \tag{14}$$

Combined with the above analysis of S-matrix, and by taking into account the propagation delay of the microstrip line TL $(\beta_1 l_1,\ \beta_2 l_2)$, the general expressions of the DGS-based BP-NGD circuit S-matrix model can be written as:

$$[S(j\omega)] = \begin{bmatrix} S_{11}(j\omega) & S_{21}(j\omega) \\ S_{21}(j\omega) & S_{11}(j\omega) \end{bmatrix} \tag{15}$$

where:

$$S_{11}(j\omega) = \frac{Z(j\omega)}{Z(j\omega) + 2Z_0} e^{-j2\beta_1 l_1} \tag{16}$$

$$S_{21}(j\omega) = \frac{2Z_0}{Z(j\omega) + 2Z_0} e^{-j(\beta_1 l_1 + \beta_2 l_2)}. \tag{17}$$

Substituting equation (14) into transmission coefficient equation (17), the DGS-based BP-NGD circuit transmission phase can be expressed as:

$$\varphi(\omega) = \left\{ \begin{array}{l} \arctan\left[\frac{a(\omega)\cos\theta(\omega) - \sin\theta(\omega)}{a(\omega)\sin\theta(\omega) + \cos\theta(\omega)}\right] \\ -\arctan\left[\frac{a(\omega)}{1+g}\right] \end{array} \right\} \tag{18}$$

with:

$$\begin{cases} \theta(\omega) = \beta_1(\omega)l_1 + \beta_2(\omega)l_2 \\ a(\omega) = \frac{(\omega^2-\omega_0^2)Q}{\omega_0\omega} \end{cases} \tag{19}$$

By means of equation (3), the corresponding GD can be written as:

$$GD(\omega) = GD_1(\omega) - GD_2(\omega) \tag{20}$$

where:

$$GD_1(\omega) = \frac{\frac{2Q}{\omega_0(1+g)} - \frac{a(\omega)Q}{\omega_0(1+g)}}{\frac{a(\omega)^2}{(1+g)^2} + 1} \tag{21}$$

$$GD_2(\omega) = \frac{\left[\frac{2Q}{\omega_0} - \frac{a(\omega)}{\omega}\right]\left[1 + \tan^2\theta(\omega)\right]}{[\tan\theta(\omega) - a(\omega)]^2 + [1 + a(\omega)\tan\theta(\omega)]^2} \tag{22}$$

3) ANALYSIS AT PARTICULAR FREQUENCIES

Similar to filters, NGD functions can also be classified according to the positioning of frequency bands. According to this, we can have BP NGD function. NGD analysis includes identifying the presence of NGD:

$$GD(\omega) < 0 \tag{23}$$

The NGD cut-off frequencies ω_1 and ω_2 can be determined as the roots of the equation:

$$GD(\omega) = 0 \tag{24}$$

and the NGD bandwidth can be formulated by:

$$\Delta\omega = \omega_2 - \omega_1 = 2\pi\,\Delta f \tag{25}$$

At the NGD centre frequency f_0 (or ω=ω_0), we have the following expressions of:

- the reflection parameter given in equation (16) becoming:

$$S_{11}(\omega)\big|_{\omega=\omega_0} = \frac{g}{1+g} \tag{26}$$

- the transmission parameter given in equation (17) becoming:

$$S_{21}(\omega)\big|_{\omega=\omega_0} = \frac{1}{1+g} \tag{27}$$

- the GD given by equation (20) simplified as:

$$GD(\omega)\big|_{\omega=\omega_0} = \frac{2Q}{\omega_0(1+g)} - \frac{2Q}{\omega_0} \tag{28}$$

Therefore, the GD is unconditionally negative around the resonance frequency $\omega = \omega_0$. At very low frequencies, the GD simplified as:

$$GD(\omega)\big|_{\omega\approx 0} = \frac{N^2R}{2QZ_0\omega_0} = \frac{g}{Q\omega_0} \tag{29}$$

is always positive for any SRR parameters. It means that the DGS-based topology under study behaves as a BP-NGD function.

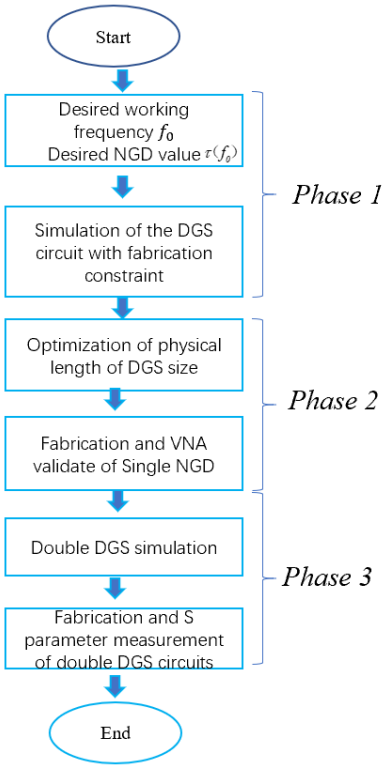

FIGURE 2. Methodological flow chart of NGD circuit design and test.

C. DESIGN AND TEST METHODOLOGY OF THE DGS-BASED BP-NGD CIRCUIT

The methodology to design and to test the BP-NGD microwave passive circuits must begin with the expected fabrication technology and the desired value of NGD value and NGD center frequency. Then, we can follow the design guideline indicated by the flow chart of Fig. 2 until the NGD circuit prototype fabrication and test. As indicated in Fig. 2, the proposed design and test method of NGD microwave passive circuit can be divided in three successive phases:

- Phase 1: At the beginning of the design, the NGD function around the expected working frequency must be specified. Then, the analytical computation can be realized based on the ideal model of the S-parameters. Some parametric analyses can also be performed in this phase in order to check the better comprehension of influence of parameters constituting the NGD topology.
- Phase 2: In this intermediate step, the NGD engineer must take care on the available technology for fabricating the NGD prototype. For example, in the present study as it will be explored in the next validation section, we will deal with microstrip technology to design and implemented our NGD prototype. Therefore, in this step, the NGD circuit can be designed with the design and simulation tools (as in the present study, we will utilize with the RF and microwave circuit ADS®designer and simulator from Keysight Technologies®). The simulations are focused on the realistic effects on the NGD

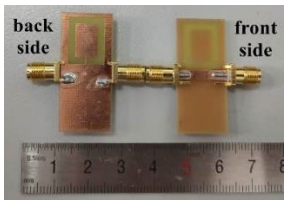

FIGURE 3. Photograph of the single wing DGS circuit prototype.

prototype. It consists of simulating and optimizing the NGD circuit by taking into account the realistic effects as the DGS size, the distance between DGS and TL. The fabrication and VNA S parameter test of single DGS NGD circuit.

- Phase 3: In this last phase, the double wing NGD prototype must be fabricated from the circuit layout drawn from the single DGS optimized design performed in Phase 2. Acting as an RF and microwave circuit, the NGD prototype can be tested with a Vector Network Analyzer (VNA). Before the tests, the VNA must be calibrated with consideration of the working frequency. The test must start with the S-parameter measurements.

To verify more realistically the efficiency of the developed NGD design method, POC of DGS circuit will be investigated in the two next sections.

III. DESIGN OF SINGLE-WING DGS TOPOLOGY

As POC prototype, a single-wing DGS circuit was designed in microstrip topology. The innovative DGS prototype was designed, simulated, fabricated and tested to verify the feasibility of the BP-NGD function. The following subsections will describe the results of design and test of the NGD circuit prototype.

A. STRUCTURAL DESCRIPTION

Fig. 3 displays top and back sides of the fabricated DGS BP-NGD prototype with size 15 mm × 32 mm. The parameters of the DGS wing were chosen and optimized in order to generate the BP-NGD specifications as NGD center frequency, f_0, between 2.4 GHz and 2.6 GHz, and NGD value of some minus nanoseconds.

The circuit is also expected to operate under low-attenuation and well access matching.

Before the discussion on feasibility study results, the fabricated prototype will be introduced in the following paragraph.

B. PRESENTATION OF THE DGS POC PROTOTYPE

The POC single wing DGS circuit was implemented Cu-metallized on FR4-based substrate. It acts as a two-port passive circuit. As shown in Fig. 1(a), the values of the physical parameters of the circuit are addressed in Table 1.

All the simulation results presented in the present paper were obtained from simulations with the 3-D electromagnetic (EM) HFSS®commercial tool from Ansys®. The measurements were carried out with a vector network analyzer (VNA) from Rohde & Schwarz®referenced ZNB 20 and specified by frequency band 100 kHz to 20 GHz.

TABLE 1. DGS microstrip circuit parameters and specifications.

Components	Description	Parameter	Value
Dielectric substrate	Material	FR4	-
	Relative permittivity	ε_r	4.6
	Loss tangent	tan(δ)	0.02
	Thickness	h	1.5 mm
Metallization	Material	Copper (Cu)	-
	Thickness	t	35 µm
	Conductivity	σ	58 MS/m
DGS NGD circuit	Total length	L	15 mm
	Total width	W	32 mm
	DGS length	l_1	10.5 mm
	DGS width	l_2	14 mm
	DGS Opening width	g	0.5 mm
	DGS line space	w_2	2 mm
	Coupling distance	d	0.8 mm
	Transmission line width	w_1	3.06 mm

TABLE 2. NGD specifications versus coupling distance, d.

d (mm)	Z (Ω)	f_0 (GHz)	$GD(f_0)$ (ns)	$S_{21}(f_0)$ (dB)
0.4	52.5	2.506	-2.05	-3.32
0.6	52.7	2.511	-1.61	-2.62
0.8	51.7	2.515	-1.13	-1.93
1.2	51.9	2.535	-0.91	-1.59
1.4	52.0	2.559	-0.86	-1.51

For the better understanding the influence of each physical dimension on the BP-NGD function, parametric analyses will be explored in the next paragraph.

C. PARAMETRIC ANALYSES WITH RESPECT TO THE DGS PHYSICAL SIZES

To check the PCB fabrication accuracy, the present parametric investigation is based on the S-parameter computation of the DGS structure introduced previously. The computations were realized in the HFSS®environment. The simulations were run withing the frequency bandwidth from 2.3 GHz to 2.7 GHz under 200 frequency sampling.

1) PARAMETRIC ANALYSIS VERSUS D

The first parametric analysis was performed by varying d from 0.4 mm to 1.4 mm and fixing all the other parameters in Table 1.

After simulations, we obtain the results cartographied by Figs. 4. It can be understood from Fig. 4(a) that the BP-NGD aspect is kept with the considered variation of d.

The changes of the BP-NGD performance are summarized in Table 2. Z is the port impedance of the DGS circuit. It can be pointed out that the NGD center frequency, f_0, increases slightly of about 53 MHz when the CSRR length, d, increases from 0.4 mm to 1 mm. Nevertheless, the GD value, defined

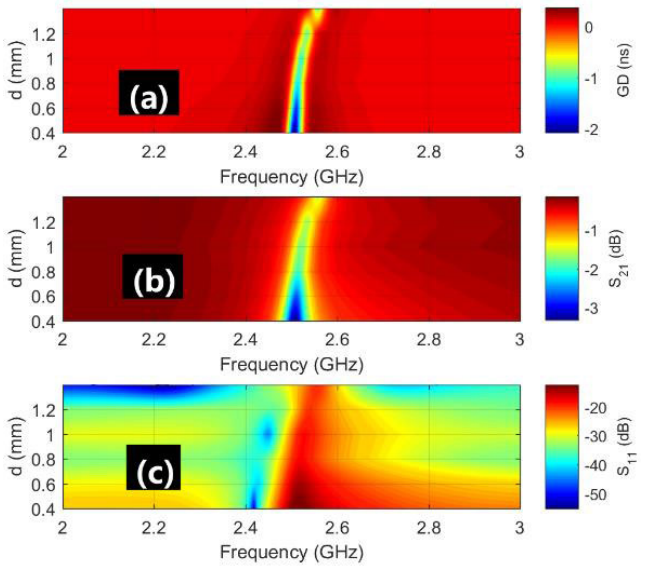

FIGURE 4. Parametric simulated results versus d: (a) GD, (b) S_{21} and (c) S_{11}.

TABLE 3. NGD specifications versus coupling distance, L_2.

L_2 (mm)	Z (Ω)	f_0 (GHz)	$GD(f_0)$ (ns)	$S_{21}(f_0)$ (dB)
13	53.2	2.62	-1.16	-2.00
13.5	53.0	2.58	-1.17	-2.00
14	51.7	2.515	-1.15	-1.92
14.5	51.9	2.47	-1.12	-1.84

in (7), varies −2.05 ns to −0.86 ns. As depicted in Fig. 4(b), the transmission coefficient given in (8) varies from −3.32 dB to −1.51 dB. Moreover, the single wing DGS structure access matching is guaranteed with reflection coefficient widely better than −15 dB in the NGD bandwidth.

2) PARAMETRIC ANALYSIS VERSUS L_2

This second parametric analysis aims to investigate the influence of L_2. This later one was varied from 13 to 14.5 mm by fixing all the other ones as shown in Table 1. The cartographies of Figs. 5 confirm the BP-NGD responses of the single wing DGS structure with respect to L_2.

Table 3 indicates the influence of this length on the BP-NGD performances.

As seen in Fig. 5(a), the NGD center frequency, f_0, is inversely proportional to L_2. However, $GD(f_0)$ is not literally sensitive to this length because the variation is almost negligible. The variation of S_{21} shown in Fig. 5(b) can be also neglected. The input and output matchings illustrated by the maps of reflection coefficients displayed in Fig. 5(c) are kept better than −15 dB with the considered range of L_2 variation.

D. SINGLE-WING DGS PROTOTYPE EXPERIMENTAL VALIDATION RESULTS

The present S-parameter measurements have been carried out for the experimental validation of the single-wing BP-NGD function with the DGS tested circuit. Figs. 6 show the comparisons between the simulated and measured results.

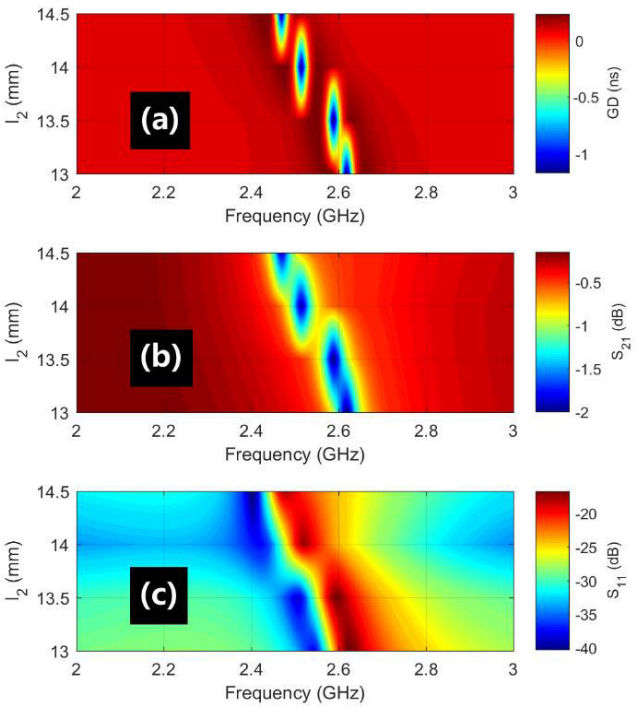

FIGURE 5. Parametric simulated results versus L_2: (a) GD, (b) S_{21} and (c) S_{11}.

TABLE 4. Simulated and experimented NGD performances of simple-wing DGS prototype shown in Fig. 7.

Validation Method	f_0 *(GHz)*	GD_n *(ns)*	*BW (MHz)*	S_{21} *(dB)*	S_{11} *(dB)*
Simulation	2.515	-1.15	41	-1.92	-17.5
Measurement	2.510	-1	30	-1.56	-16.7

As expected, these well-correlated results validate the single-wing DGS POC BP-NGD function.

Table 4 summarizes the comparison of NGD performances from the simulation, calculation and measurement. As plotted in Fig. 6(a), at the center frequency, $f_0 = 2.5$ GHz, the tested circuit present the NGD optimal simulated and measurement values, $GD(f_0)$, approximately −1.15 ns against −1 ns, respectively. The NGD bandwidth is approximately 31 MHz.

As shown in Fig. 5(b) and Fig. 6(c), the transmission coefficient is equal to −1.56 dB while the reflection coefficient is better than −16.7 dB within the NGD bandwidth. The differences between the simulated and experimental results are slight.

The parameter value of the equivalent circuit shown in Figs. 1(b) used in the calculation result is: $R_1 = 39.3\ \Omega$, $C_1 = 127.5$ pF, $L_1 = 31$ pH and $N = 0.58$.

IV. BP-NGD DESIGN AND TEST OF DOUBLE-WING DGS PROTOTYPE

It can be underlined from the previous study that the BP-NGD performance of single-wing DGS NGD circuit could be potentially improved by multiplying the number of CSRR wings on the same circuit. To confirm the veracity of this

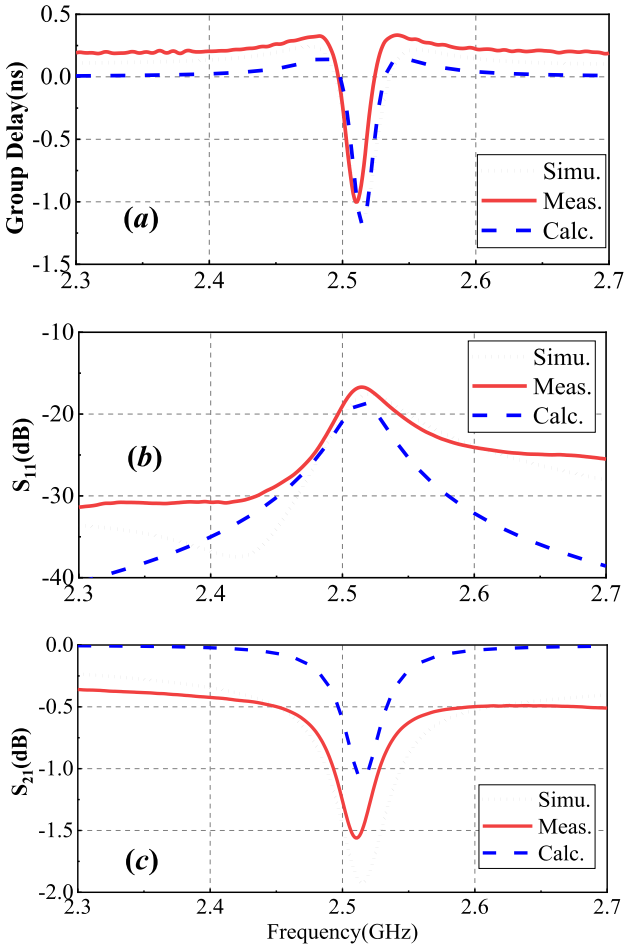

FIGURE 6. Simulated, calculated and measured (a) GD, (b) S_{11} and (c) S_{21} of single-wing DGS BP-NGD prototype.

curious thinking, a designability of double-wing DGS NGD circuit was investigated.

A. DESIGN DESCRIPTION OF DOUBLE-WING DGS POC

The prototype of double-wing DGS structure is shown in Fig. 7. As seen in Fig. 7(a), compared to the previous case of single wing, the present DGS POC consists of two CSRR wings.

Each wing has the same physical parameters as the single wing circuit shown in Fig. 1, which are placed at distance, d, in left and right of the microstrip line. The addition of double wind NGD circuit does not increase the physical size of the total circuit when compared with single wing NGD circuit. The proof of concept (POC) double wing DGS circuit was implemented Cu-metallized on FR4-based substrate. It acts as a two-port passive circuit. Fig. 6(b) displays top and back sides of the fabricated prototype with physical size 15 mm $\times$ 32 mm.

B. SIMULATED AND EXPERIMENTAL VALIDATION RESULTS

The S-parameters of the two-wing DGS circuit prototype were measured from 2.3 GHz to 2.7 GHz. Figs. 7 show the

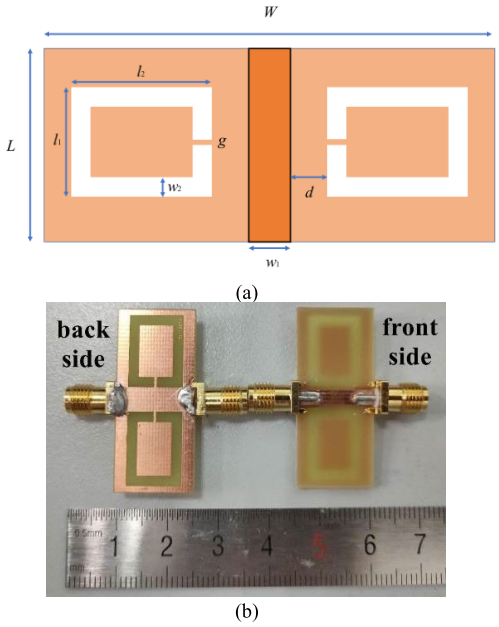

FIGURE 7. Double wing DGS planar design: (a) top view of the overall circuit and (b) photograph of the double wing DGS circuit prototype.

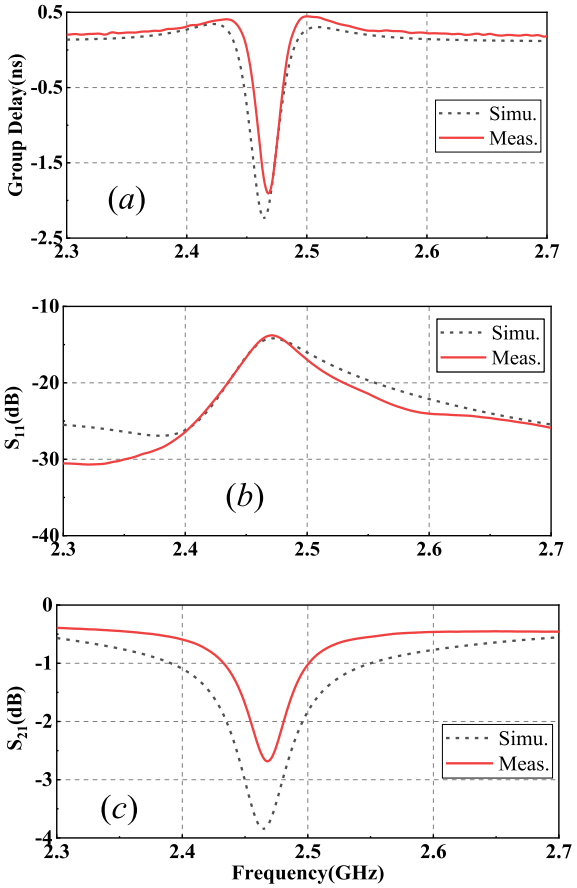

FIGURE 8. Simulated and measured (a) GD, (b) S_{11} and (c) S_{21}.

comparisons between the obtained simulated and measured results. The comparison of associated NGD performances generated from simulation and measurement are tabulated

TABLE 5. Simulated and experimented NGD performances of double-wing DGS prototype shown in Figs. 6.

Validation method	f_0 (GHz)	GD_n (ns)	BW (MHz)	S_{21} (dB)	S_{11} (dB)
Simulation	2.464	-2.46	48.4	-3.85	-14.2
Measurement	2.468	-1.9	35	-2.68	-13.81

TABLE 6. Comparison of BP-NGD performances.

References	f_0 (GHz)	GD_n (ns)	BW (MHz)	S_{21} (dB)	S_{11} (dB)	Size (λ_g^2)
[12]	3.50	-3.8	100	-37.1	*	0.89*0.27
[13]	1.00	-2.06	40	-7.8	-25.7	0.53*0.30
[14]	1.00	-2.02	69	-6.5	-11.3	0.18*0.25
[23]	2.90	-0.9	43	-2.2	-13	0.93*0.46
[24]	3.10	-4.8	15	-2.87	-11.8	1.1*0.57
[25]	1.89	-1	20	-1.7	-15	1.1*0.49
This work	2.46	-1.9	35	-2.68	-14	0.47*0.22

* No data in the origin references, simulation results indicate it is not better than -10 dB.

in Table 5. Compared to single-wing DGS NGDC previously analyzed, the double wing circuit NGD value stated in Fig. 7(a) is increased from −1 ns to −1.9 ns.

Nevertheless, the NGD bandwidth is increased from 30 MHz to 35 MHz. The double-wing DGS prototype transmission coefficient defined in (8) plotted in Fig. 7(b) is equal to −2.68 dB.

The tested reflection coefficient displayed in Fig. 7(c) is better than 13.8 dB. The largest differences between the simulated and experimental results on transmission coefficient is about 1.17 dB. It is due to the numerical computation inaccuracies, the substrate dispersion loss, the metallization skin effect, and the fabricated circuit imperfection as the connector solder in the considered working frequency.

Through the design and verification of double wing DGS circuit, multi-unit DGS circuit is feasible. Larger NGD value and multi-band NGD circuit can be obtained by etching multiple DGS units on the ground behind the microstrip line.

C. DISCUSSION ON NGD PERFORMANCES AND POTENTIAL APPLICATIONS

Table 6 reports the comparisons between the BP-NGD performances of the designed DGS-based NGD circuit with the results available in the literature [12], [13], [14] and the previous work [23], [24], [25]. It is interesting to note that compared to the DGS BP-NGD circuit introduced in [12], the developed double-wing one presented in this paper show considerable advantages in terms of insertion and size. Furthermore, compared to other BP-NGD circuits as introduced in [13], [14], [23], [24], and [25], those BP-NGD circuits is usually connected to both ends of the circuit to be balanced in cascaded form. The microstrip resonant structure will take up too much space on the PCB board and cause radiation interference to other transmission lines. The proposed DGS BP-NGD topology presents a lower attenuation loss with considerable compact physical size. The design simplicity and the fabrication parameter degree of freedom make the developed DGS BP-NGD topology as a best candidate for the future microwave communication devices.

One can cite various applications as 5-G devices in terms of design simplicity which is potentially integrable in different RF/microwave functions, design miniaturization, BP-NGD SWaP improvement, and notably for the GD and signal delay equalization with the possibility to implement the structure on the back side of the PCB. The proposed DGS BP-NGD topology can also be used in terms of progressive phase delay, such as passive beam steering [21] and return loss improvement [22].

V. CONCLUSION

An investigation of BP-NGD designing of innovative microwave circuit including a CSRR wing-based DGS topology is developed. The passive DGS-topology is composed of fully passive distributed elements with a TL and two identical wings at back side.

The relevance of the BP-NGD design study was verified by simulations and measurements of different microstrip prototypes. Parametric analyses were conducted in function of the CSRR physical parameters. The BP-NGD performances of the DGS-topology around the 2.4-GHz expected operation frequency were investigated with 2-D cartographies. More importantly, comparisons between the simulated and measured results are also discussed. Furthermore, excellent agreement between simulations and measurements of single- and double-wing DGS prototypes is confirmed with the BP-NGD behavior.

In the future, because of the design simplicity and the increase of NGD performances, the proposed NGD DGS topology open potential applications of BP-NGD function notably in the area of RF and microwave telecommunication engineering.

REFERENCES

[1] H. Choi, Y. Jeong, C. D. Kim, and J. S. Kenney, "Efficiency enhancement of feedforward amplifiers by employing a negative group delay circuit," *IEEE Trans. Microw. Theory Techn.*, vol. 58, no. 5, pp. 1116–1125, May 2010.

[2] H. Noto, K. Yamauchi, M. Nakayama, and Y. Isota, "Negative group delay circuit for feed-forward amplifier," in *IEEE MTT-S Int. Microw. Symp. Dig.*, Jun. 2007, pp. 1103–1106.

[3] S. Keser and M. Mojahedi, "Removal of beam squint in series fed array antennas using abnormal group delay phase shifters," in *Proc. IEEE Antennas Propag. Soc. Int. Symp.*, Jul. 2010, pp. 1–4.

[4] H. Mirzaei and G. V. Eleftheriades, "Arbitrary-angle squint-free beamforming in series-fed antenna arrays using non-Foster elements synthesized by negative group delay networks," *IEEE Trans. Antennas Propag.*, vol. 63, no. 5, pp. 1997–2010, May 2015.

[5] A. Taslimi, W. Alomar, and A. Mortazawi, "Phase compensated serially fed array using the antenna as a part of negative group delay circuit," in *IEEE MTT-S Int. Microw. Symp. Dig.*, May 2015, pp. 1–4.

[6] D.-J. Woo and T.-K. Lee, "Suppression of harmonics in Wilkinson power divider using dual-band rejection by asymmetric DGS," *IEEE Trans. Microw. Theory Techn.*, vol. 53, no. 6, pp. 2139–2144, Jun. 2005.

[7] C. Kumar and D. Guha, "Reduction in cross-polarized radiation of microstrip patches using geometry-independent resonant-type defected ground structure (DGS)," *IEEE Trans. Antennas Propag.*, vol. 63, no. 6, pp. 2767–2772, Jun. 2015.

[8] S. Hekal, A. B. Abdel-Rahman, H. Jia, A. Allam, A. Barakat, and R. K. Pokharel, "A novel technique for compact size wireless power transfer applications using defected ground structures," *IEEE Trans. Microw. Theory Techn.*, vol. 65, no. 2, pp. 591–599, Feb. 2017.

[9] C. Kumar and D. Guha, "Asymmetric and compact DGS configuration for circular patch with improved radiations," *IEEE Antennas Wireless Propag. Lett.*, vol. 19, no. 2, pp. 355–357, Feb. 2020.

[10] G. Chaudhary, Y. Jeong, and J. Lim, "Miniaturized dual-band negative group delay circuit using dual-plane defected structures," *IEEE Microw. Wireless Compon. Lett.*, vol. 24, no. 8, pp. 521–523, Aug. 2014.

[11] G. Chaudhary, J. Jeong, P. Kim, Y. Jeong, and J. Lim, "Compact negative group delay circuit using defected ground structure," in *Proc. Asia–Pacific Microw. Conf. Proc. (APMC)*, Seoul South Korea, Nov. 2013, pp. 22–24.

[12] B. Ravelo, *Negative Group Delay Devices: From Concept to Applications* (IET Materials, Circuit and Devices Series), vol. 43. London, U.K.: Publisher Michael Faraday House, 2018.

[13] Z. Zhu, Z. Wang, S. Zhao, H. Liu, and S. Fang, "A novel balanced-to-unbalanced negative group delay power divider with good common-mode suppression," *Int. J. RF Microw. Comput.-Aided Eng.*, vol. 32, no. 7, Jul. 2022, Art. no. e23173, doi: 10.1002/mmce.23173.

[14] Y. Meng, Z. Wang, S. Fang, and H. Liu, "Reconfigurable negative group delay circuit with tunable group delay flatness," *Int. J. RF Microw. Comput.-Aided Eng.*, vol. 32, no. 6, pp. 42–46, Jun. 2022.

[15] L.-F. Qiu, L.-S. Wu, W.-Y. Yin, and J.-F. Mao, "Absorptive bandstop filter with prescribed negative group delay and bandwidth," *IEEE Microw. Wireless Compon. Lett.*, vol. 27, no. 7, pp. 639–641, Jul. 2017.

[16] Z. Wang, Y. Cao, T. Shao, S. Fang, and Y. Liu, "A negative group delay microwave circuit based on signal interference techniques," *IEEE Microw. Wireless Compon. Lett.*, vol. 28, no. 4, pp. 290–292, Apr. 2018.

[17] C.-T. M. Wu and T. Itoh, "Maximally flat negative group-delay circuit: A microwave transversal filter approach," *IEEE Trans. Microw. Theory Techn.*, vol. 62, no. 6, pp. 1330–1342, Jun. 2014.

[18] T. Shao, Z. Wang, S. Fang, H. Liu, and S. Fu, "A compact transmission line self-matched negative group delay microwave circuit," *IEEE Access*, vol. 5, pp. 22836–22843, 2017.

[19] T. Shao, S. Fang, Z. Wang, and H. Liu, "A compact dual-band negative group delay microwave circuit," *Radioengineering*, vol. 27, no. 4, pp. 1070–1076, Dec. 2018.

[20] X. Zhou, B. Li, N. Li, B. Ravelo, X. Hu, Q. Ji, F. Wan, and G. Fontgalland, "Analytical design of dual-band negative group delay circuit with multi-coupled lines," *IEEE Access*, vol. 8, pp. 72749–72756, 2020.

[21] M. U. Afzal, L. Matekovits, K. P. Esselle, and A. Lalbakhsh, "Beam-scanning antenna based on near-electric field phase transformation and refraction of electromagnetic wave through dielectric structures," *IEEE Access*, vol. 8, pp. 199242–199253, 2020.

[22] A. Ahmadi, S. V. Makki, A. Lalbakhsh, and S. Majidifar, "A novel dual mode wide band bandpass filter," *Appl. Comput. Electromagn. Soc. J.*, vol. 29, no. 9, pp. 735–742, 2014.

[23] F. Wan, B. Liu, P. Thakur, A. Thakur, S. Lallechere, W. Rahajandraibe, and B. Ravelo, "0IO-shape PCB trace negative group-delay analysis," *IEEE Access*, vol. 8, pp. 97707–97717, 2020.

[24] B. Ravelo, F. Wan, S. Lallechere, G. Fontgalland, and W. Rahajandraibe, "Design and test of crab-shaped negative group delay circuit," *IEEE Design Test*, vol. 39, no. 1, pp. 67–76, Feb. 2022.

[25] F. Wan, N. Li, B. Ravelo, W. Rahajandraibe, and S. Lallechere, "Design of =I= shape stub-based negative group delay circuit," *IEEE Design Test*, vol. 38, no. 2, pp. 78–88, Apr. 2021.

QIZHENG JI received the M.S. degree in aircraft design from the China Academy of Space Technology (CAST), Beijing, China, in 2006. He is currently working toward the Ph.D. degree from Army Engineering University, Shijiazhuang Campus, National Key Laboratory on Electromagnetic Environment Effects, China. He is currently a Professorate Senior Engineer with the Beijing Institute of Spacecraft Environment Engineering, Beijing. His research interests include microwave circuits and ESD.

TAOCHEN GU (Student Member, IEEE) received the B.Sc. degree in electrical engineering from the Nanjing University of Information Science and Technology, Nanjing, China, in 2018, where he is currently pursuing the Ph.D. degree. His research interests include abnormal wave propagation in dispersive media and microwave circuits.

ZHILIANG GAO received the M.S. degree in automated testing and control from the Harbin Institute of Technology, China, in 2011. He is currently a Senior Engineer in technology and management of electrostatic protection with the Beijing Orient Institute of Measurement and Test, CAST, Beijing, China.

MING YANG received the B.S. and Ph.D. degrees in microelectronics from Shandong University, Jinan, China, in 2011 and 2016, respectively. He is currently an Engineer with the Beijing Orient Institute of Measurement and Test, Chinese Academy of Space Technology, Beijing, China. His current research interests include the microelectronic devices and the electrostatic technology.

YAFEI YUAN received the M.S. degree in spacecraft design from the Chinese Academy of Space Technology (CAST), Beijing, China, in 2007. He is currently a Professor of engineering in technology and management of electrostatic protection with the Beijing Orient Institute of Measurement and Test, CAST.

HONGYU DU (Student Member, IEEE) received the B.Eng. degree in communication engineering from the Nanjing University of Information Science and Technology, Nanjing, China, in 2018, where she is currently pursuing the Ph.D. degree. Her research interests include negative group delay mechanism and complex permittivity measurement technology.

FAYU WAN (Senior Member, IEEE) received the Ph.D. degree in electronic engineering from the University of Rouen, Rouen, France, in 2011. From 2011 to 2013, he was a Postdoctoral Fellow with the Electromagnetic Compatibility Laboratory, Missouri University of Science and Technology, Rolla. He is currently a Full Professor with the Nanjing University of Information Science and Technology, Nanjing, China. His current research interests include negative group delay circuits, electrostatic discharge, electro-magnetic compatibility, and advanced RF measurement.

NOUR MOHAMMAD MURAD (Member, IEEE) was born in Saint Denis, La Réunion, France, in 1974. He received the Ph.D. degree in communication and electronics from the Ecole Nationale Supérieure des Télécommunications (Telecom Paris), in 2001. From 1998 to 2001, he served as a Research and Development Engineer with Alcatel CIT. During this period, he prepared his doctoral thesis with Télécom Paris. From 2001 and 2003, he worked as a Teacher and a Researcher with the University of La Réunion, where he had co-responsibility on the coupling between energy and telecommunication project. From 2004 to 2007, he was a Research Assistant Professor with the 3IL Engineering School and a Researcher with XLIM/OSA (Limoges University). Since September 2007, he has been a Research Assistant Professor with the University of Réunion. In 2018, he obtained his Accreditation to Direct Research (HdR) in numerical communications and networks. He became an Associate Professor, in 2019, and was responsible of a team research on ''Energy Optimization for Sensor Networks'' (five researchers). He has directed and co-supervised five Ph.D. and four master's students. He was the scientific co-responsible of projects, titled ORIANA ANR and FEDER CARERC. It's research relates to the numerical communication and RF, signal and information theory, with a specific accent on wireless communications, spread spectral techniques, synchronization, MIMO systems, techniques diversity, wireless energy transportation, antenna networks, and wireless sensor networks.

GLAUCO FONTGALLAND (Senior Member, IEEE) was born in Fortaleza, Brazil, in March 1966. He received the degree and M.S. degrees in electrical engineering from the Universidade Federal de Campina Grande (UFCG), Campina Grande, Brazil, in 1990 and 1993, respectively, and the Ph.D. degree in electronics from the Toulouse Institute National Polytechnique–ENSEEIHT, Toulouse, France, in 1999. From 2010 to 2012, he was a Visiting Scholar with the ElectroScience Laboratory, Ohio State University (OSU), USA. Currently, he is a Full Professor with the UFCG, where he develops research on: electromagnetic modeling, EMC, EMI, ESD, RFID, UWB, propagation, and antennas for various applications. He has published more than 200 papers in journals and conferences. He is a member of the Sociedade Brasileira de Micro-ondas e Optoeletrônica (SBMO), Sociedade Brasileira de Eletromagnetismo (SBMag), Sociedade Brasileira de Microeletrôncia (SBMicro), and the Applied Computacional Eletromagnetics Society (ACES). He is also the past IEEE AP-S chapter Chair and a member of the 2020 IEEE AP-S Student Design Contest and 2020 IEEE AP-S Field Awards Evaluation. His Thesis work was nominated for the Leopold Escande Award 1999. Since 2019, he has been an Associate Editor of IEEE Latin America Transactions.

HUGERLES S. SILVA (Member, IEEE) received the B.Sc., M.Sc., and Ph.D. degrees in electrical engineering from UFCG, Brazil, in 2014, 2016, and 2019, respectively. Currently, he is a Postdoctoral Student with the Telecommunications Institute, University of Aveiro, Portugal. His main research interests include wireless communication, digital signal processing, and wireless channel modeling.

BLAISE RAVELO (Member, IEEE) is currently a University Full Professor with NUIST, Nanjing, China. He is a Lecturer of circuit and system theory, STEM (science, technology, engineering and maths), and applied physics. He is a Pioneer of the negative group delay (NGD) concept, theory, design, fabrication, test, and applications. This extraordinary concept is potentially useful for anticipating and prediction all kind of information. He was a research director of 11 Ph.D. students (ten defended), postdocs, research engineers, and master's internships. With U.S., Chinese, Indian, European, and African partners, he is actively involved and contributes on several international research projects. He is the (co) author of more than 390 scientific research papers in new technologies published in international conference and journals. His research interests include multiphysics and electronics engineering. He is a member of Scientific Technical Committee of Advanced Electromagnetic Symposium (AES). He is also a member of research groups: URSI, GDR Ondes, and Radio Society. He is ranked in Top 2% world's scientists based on years (2020–2022) by Stanford University, USA. He has Google Scholar H-index (2023) is 27 and i10-index (2023) is 84. He is regularly invited to review papers submitted for publication to international journals, such as IEEE Transactions on Microwave Theory and Techniques, IEEE Transactions on Circuits and Systems, IEEE Transactions on Electromagnetic Compatibility, IEEE Transactions on Industrial Electronics, IEEE Access, *IET CDS*, and *IET MAP*; and books (Wiley and Intech Science). He is a member of *IET Electronics Letters* Editorial Board as circuit and system subject editor.